HTML ABSTRACT • LINKS

Photoconductivity decay in metamorphic InAsP/InGaAs double heterostructures grown on $InAs_yP_{1-y}$ compositionally step-graded buffers

Y. Lin and M. K. Hudait
Department of Electrical and Computer Engineering, The Ohio State University, Columbus, Ohio 43210

S. W. Johnston and R. K. Ahrenkiel
National Renewable Energy Laboratory, Golden, Colorado 80401

S. A. Ringel[a]
Department of Electrical and Computer Engineering, The Ohio State University, Columbus, Ohio 43210

(Received 27 September 2004; accepted 20 December 2004; published online 9 February 2005)

Lattice-mismatched $InAs_{0.32}P_{0.68}/In_{0.68}Ga_{0.32}As/InAs_{0.32}P_{0.68}$ double heterostructures (DH) were grown on compositionally graded $InAs_yP_{1-y}$/InP substrates by solid-source molecular-beam epitaxy (MBE) out to a misfit of ~1%. The kinetics of carrier recombination were investigated in the nearly totally relaxed MBE-grown DH structures using photoconductivity decay (PCD) measurements. High minority carrier lifetimes of 4–5 μs close to the radiation limit were measured, indicating the ability of MBE-grown $InAs_yP_{1-y}$ buffers in achieving high-electronic-quality, low-band-gap mismatched InGaAs layers. Analysis suggests that very low interface recombination velocities are achieved. A photogenerated carrier diffusion model is presented to explain the initial nonlinear decays observed in PCD data for these heterostructures. © *2005 American Institute of Physics*. [DOI: 10.1063/1.1866645]

High In-content (>53% In), low-band-gap InGaAs is receiving a great deal of attention due to its potential for applications ranging from ultrahigh speed electronics to infrared optoelectronics and thermophotovoltaic (TPV) devices.[1–5] To obtain the level of material quality necessary for device applications requires an intermediate buffer to transition from a common substrate, in this case InP, to a lattice constant that matches that of the low-band-gap InGaAs. $InAs_yP_{1-y}$ alloys are ideally suited for this application, with lattice constants spanning from InP to InAs. Moreover for molecular-beam epitaxy (MBE) growth, the use of the anion sublattice to adjust the lattice constant is advantageous since this decouples the introduction of lattice misfit from the growth rate. Recently, MBE-grown $InAs_yP_{1-y}$ step-graded buffers graded out to $InAs_{0.4}P_{0.6}$ on InP, a 1.3% total misfit, have yielded low threading dislocation densities in the $\sim 4 \times 10^6$ cm^{-2} range, very low surface roughness and no evidence for branch defects that have been observed in InGaAs, InAlAs, and InGaP cation graded buffers.[6,7] Preliminary, lattice-mismatched InGaAs TPV devices grown on graded $InAs_yP_{1-y}$ buffers/InP substrates using MBE have yielded performance comparable to metalorganic chemical vapor deposition (MOCVD)-grown TPV cells of similar design, with extremely high lateral uniformity.[4,5] However there have been no reports on the minority carrier lifetime and carrier recombination kinetics in MBE-grown mismatched InGaAs on InP, and this information is necessary to identify carrier loss mechanisms so that MBE-grown mismatched InGaAs/InAsP/InP heterostructures can be optimized and better understood. This letter presents such a study for metamorphic InGaAs/InAsP/InP heterostructures grown by MBE. Very high carrier lifetimes are observed for InGaAs layers with ~1% misfit and a model is presented to account for the full nature of the photoconductivity decay (PCD) response typically used to obtain quantitative lifetime values from these materials.

$InAs_{0.32}P_{0.68}/In_{0.68}Ga_{0.32}As/InAs_{0.32}P_{0.68}$ double heterostructures (DH) were grown in a solid-source MBE system equipped with valved cracker cells for both arsenic (As) and phosphorus (P). The molecular forms of As and P used in the growth were As_2 and P_2, respectively. The DH structure is schematically shown in Fig. 1. All samples were grown on semi-insulating (001) InP substrates and the entire structure was unintentionally doped. Before the DH growth, a 2000 Å InP buffer was deposited, followed by an $InAs_yP_{1-y}$ compositionally step-graded buffer consisting of four steps, each of 4000 Å thickness, with compositions shown in Fig. 1. A nominal substrate temperature of 485 °C was maintained during growth of all layers as determined by optical pyrometry. The misfit between the final step in the buffer ($InAs_{0.32}P_{0.68}$) and the InP substrate is ~1%. Triple-axis x-ray diffraction (TAXRD) confirmed that >90% strain relaxation was achieved with this buffer design. Complete de-

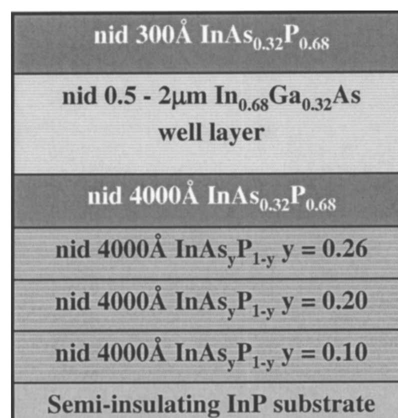

FIG. 1. Schematic cross section of metamorphic InAsP/InGaAs/InAsP double heterostructures grown on semi-insulating InP substrates using $InAs_yP_{1-y}$ step-graded buffers. All epitaxial layers are nonintentionally doped (nid) and within the doping range of $1-2 \times 10^{15}$ cm^{-3} (n type).

[a]Author to whom correspondence should be addressed; electronic mail: ringel.5@osu.edu

 © 2005 American Institute of Physics
Downloaded 01 Nov 2005 to 134.134.136.2. Redistribution subject to AIP license or copyright, see http://apl.aip.org/apl/copyright.jsp

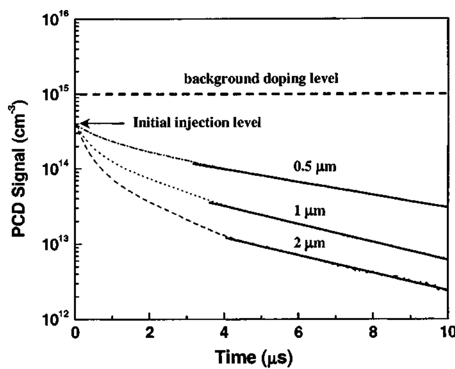

FIG. 2. PCD data obtained for DHs with well thicknesses of 0.5, 1, and 2 μm at 300 K. The solid lines are data fits to the LLI regime of the PCD response.

tails of the $InAs_yP_{1-y}$ buffer growth and relaxation properties have been reported elsewhere.[6,8] Following the buffer growth, a series of $InAs_{0.32}P_{0.68}/In_{0.68}Ga_{0.32}As/InAs_{0.32}P_{0.68}$ DH structures with InGaAs well thicknesses of 0.5, 1, and 2 μm were grown on the $InAs_yP_{1-y}$ buffers, achieving a nominal lattice-matched condition with the final $InAs_{0.32}P_{0.68}$ step of the buffer. Each DH structure included a 300 Å top $InAs_{0.32}P_{0.68}$ barrier layer to complete the DH structure. All samples were characterized using reflection high-energy electron diffraction (RHEED) to investigate the *in situ* surface structure of samples. Strong (2×4) RHEED patterns were obtained throughout the growth of each structure, indicating ideal two-dimensional growth. Uniform, two-dimensional surface cross-hatch patterns were observed for all samples by Nomarski microscopy, as expected for effective strain relaxation via $InAs_yP_{1-y}$ compositionally step-graded buffers.[6,8–11] The alloy composition of the $In_xGa_{1-x}As$ well within each DH structure was confirmed by TAXRD to be $In_{0.68}Ga_{0.32}As$ with a strain relaxation of 86% ±2% for all samples. Ultrahigh frequency photoconductive decay (UHFPCD) measurements at room temperature were made on all DH structures to monitor the photoconductivity decay within the InGaAs wells in order to gain insight into the carrier recombination in these DH structures. A range of excitation wavelength was used as described in the following. By fitting the decay after the optical excitation pulse was removed, PCD lifetimes were quantified. Complete details of this technique can be found elsewhere.[12]

Figure 2 shows PCD data obtained for 0.5-, 1-, and 2-μm-thick DH structures. The wavelength of the excitation pulse selected in the measurement was 2000 nm (0.62 eV), slightly higher than the band gap of the $In_{0.68}Ga_{0.32}As$ well layer (0.60 eV) and below the $InAs_{0.32}P_{0.68}$ band gap (1.0 eV), in order to confine band-absorbed photocarrier generation within the InGaAs wells. The incident photon flux of the excitation pulse was $\sim 2\times 10^{10}$ photons/cm^2. Assuming an absorption coefficient 2×10^4 cm^{-1} for the $In_{0.68}Ga_{0.32}As$ well layer at the wavelength of 2000 nm,[13] the 1/e penetration depth of 2000 nm photons inside the InGaAs well layer is ~ 0.5 μm. Based on these data, the initial injection level is calculated to be $\sim 4\times 10^{14}$ cm^{-3}, which can be considered equal to the initial photogenerated carrier concentration, assuming the quantum efficiency is 100%. Since the photoconductivity can be expressed as

$$\Delta\sigma = q\mu\Delta n, \tag{1}$$

where q is the electronic charge, μ is the photogenerated carrier mobility, and Δn is the concentration of photogenerated carriers, the PCD signal is proportional to the concentration of photogenerated carriers so that the initial injection level can also be considered as the starting value of the PCD curve. The unintentional background doping of the InGaAs well layer was n type $\sim 1\times 10^{15}$ cm^{-3}, which was determined by electrochemical capacitance–voltage profiling. In Fig. 2, the initial injection level and the background doping values are indicated. Fitting the low level injection (LLI) regime of PCD data denoted by the solid line fitting in Fig. 2, LLI PCD lifetimes (τ_{PCD}) were determined to be ~5, 4, and 4 μs for 0.5-, 1-, and 2-μm-thick InGaAs well DH structures, respectively. These decay lifetimes are close to the results obtained from similar DH structures grown by MOCVD.[14] The lack of dependence of lifetimes on DH well layer thickness implies a low recombination velocity, S, at the InAsP/InGaAs interfaces such that the usual expression from which the bulk minority carrier lifetime in the InGaAs well, τ_B, can be extracted according to

$$\frac{1}{\tau_{PCD}} = \frac{1}{\tau_B} + \frac{2S}{d} \tag{2}$$

is no longer valid. That is, for $S \ll d/2\tau_B$, we have $1/\tau_{PCD} \approx 1/\tau_B$. For this reason, we can consider the 4–5 μs LLI PCD lifetime to reasonably approximate the minority carrier lifetime in the bulk, relaxed InGaAs layer. Note that the PCD lifetime values are close to the band–band radiation lifetime limit of ~7 μs expected for n-InGaAs at this doping concentration and band gap, which assumes the radiative recombination coefficient to be 1.43×10^{-10} cm^3 s^{-1}.[14] These results indicate that the high quality (low dislocation density and low roughness) of the relaxed MBE-grown $InAs_yP_{1-y}$ step-graded buffers reported previously[6] translates into high-electronic-quality, mismatched InGaAs on InP with high carrier lifetime and low interface recombination velocity.

It is clear from the PCD behavior shown in Fig. 2 that the carrier recombination does not yield single-slope exponential decays as expected for ideal UHFPCD measurements. The fast initial decay observed for all three DH structures may be explained by several phenomena. First, a high value for S at the upper InAsP/InGaAs interface can yield multiexponential photoconductivity decay due to the higher concentration of photogenerated carriers near the upper interface that would dominate the initial part of the photoconductivity decay. However, the observed lack of DH thickness dependence by PCD lifetimes from Fig. 2 demonstrates that the influence of interface recombination is negligible (i.e., interface recombination is very low), eliminating this possibility. A second plausible explanation then is photogenerated carrier diffusion that can occur during the transient time window observed here as a result of the initially nonuniform carrier generation profile that is dictated by the absorption coefficient of the InGaAs layer at the excitation wavelength. The nonuniform concentration profile induces minority carrier diffusion in the InGaAs layer until an equilibrium concentration distribution is reached throughout the InGaAs layer. Once a uniform carrier distribution is reached, the photoconductivity decay becomes dominated by carrier recombination and the PCD curve becomes a steady decay curve from which the carrier recombination lifetime can be derived.

To establish the reasonableness of this explanation, the diffusion relaxation time, which is defined as the characteristic time for the diffusion process to be complete, can be

Downloaded 01 Nov 2005 to 134.134.136.2. Redistribution subject to AIP license or copyright, see http://apl.aip.org/apl/copyright.jsp

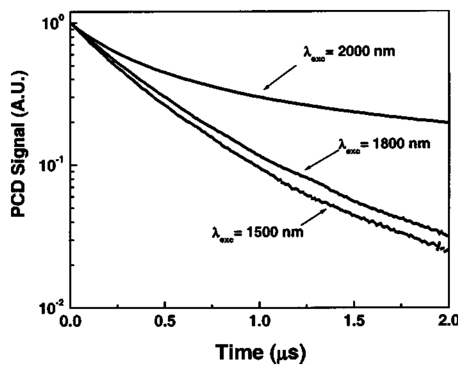

FIG. 3. The initial PCD data from 0 to 2 μs after excitation pulses with wavelength of 1500, 1800, and 2000 nm for the 2-μm-thick InGaAs well layer DH. The initial values of all curves are normalized for clearer comparison. Note the short scale compared with Fig. 2.

roughly estimated if we consider a simple diffusion model in which the initial $(t=0)$ concentration profile of photogenerated carriers $C(x,0)$, is approximated by

$$C(x, \quad 0) = C_0, 0 \leq x \leq h,$$
$$C(x, \quad 0) = 0, h < x \leq l. \tag{3}$$

In this expression, h represents the absorption depth of incident photons entering the InGaAs well layer in the PCD experiment and l is the thickness of InGaAs well layer. For the purpose of estimation, we assume $\partial C/\partial x=0$ at the boundaries and only one reflection occurs at the lower InGaAs/InAsP interface for diffusing carriers. Under these simplifying conditions, the carrier concentration $C(x,t)$ can be written as

$$C(x,t) = \frac{1}{2}C_0\left\{\text{erf}\,\frac{h-x}{2\sqrt{Dt}} + \text{erf}\,\frac{h+x}{2\sqrt{Dt}} + \text{erf}\,\frac{h+2l-x}{2\sqrt{Dt}} + \text{erf}\,\frac{h-2l+x}{2\sqrt{Dt}}\right\}, \tag{4}$$

where D is the diffusion constant of electrons in this case.[15] Since the carrier concentration $C(x,t)$ is a sum of error functions, it is expected that the dependence of $C(x,t)$ on t should not be linear on a log C-t plot, which is consistent with the initial part of the measured PCD data in Fig. 2. If we use a value for the electron mobility in $In_{0.68}Ga_{0.32}As$ layer of $6000\ cm^2/V\ s$ based on mobility data measured in MBE-grown mismatched InGaAs with similar composition and doping concentration, a diffusion relaxation time for the 2-μm-thick DH is estimated to be $\sim 5\ \mu s$. Given the simplifying approximations used in this demonstration and that the diffusion relaxation time characterizes *completion* of the diffusion process, this time is consistent with the initial decay period prior to the dominance of LLI recombination-limited decay in Fig. 2. It should be noted, however, that due to the absorption depth approximation employed, this simplified model cannot be used to determine the diffusion relaxation time for DH structures with well thickness less than the absorption depth calculated, such as for the 0.5 μm DH.

Additional support for this argument is provided by Fig. 3, which compares only the initial (0–2 μs) PCD response of the 2-μm-thick DH sample as a function of excitation wavelength at 1500, 1800, and 2000 nm. For diffusion to be important in the PCD behavior, the different initial concentration gradients that result from the dependence of the carrier generation profile on the wavelength-dependent absorption coefficient should be evident. Hence progressively reduced diffusion should be observed for increasing wavelengths (lower absorption coefficient). This trend is clearly seen in Fig. 3 for the three excitation wavelengths. The 1500 and 1800 nm excitation produce substantially larger diffusion enhanced decay in overall photoconductivity, as measured by the magnitude of PCD reduction in this nonlinear 0–2 μs regime, compared to the PCD response in the same time window using near band gap (2000 nm) excitation (note that 2000 nm corresponds to 0.62 eV and the $In_{0.68}Ga_{0.32}As$ band gap is measured to be 0.60 eV). From this, we conclude that a diffusion process that influences the overall PCD magnitude is consistent with the observed nonlinear decay in the PCD response of these materials.

In summary, high PCD recombination lifetimes of 4–5 μs have been demonstrated for ~1% mismatched InGaAs on InP using $InAs_yP_{1-y}$ step-graded buffers. In addition, outstanding interface quality is demonstrated in this mismatched heterostructure such that the InAsP/InGaAs interface recombination velocity S is low to the point where DH thickness dependence of net PCD lifetimes is not observed. A simple model combined with wavelength-dependent analysis of the initial nonlinear decay observed in PCD data is presented to explain the possible role of carrier diffusion in PCD characterization of mismatched InGaAs/InP grown by MBE.

This work was supported by National Science Foundation under Grant Nos. DMR-0076362 and DMR-0313468.

[1] K. Shinohara, Y. Yamashita, A. Endoh, I. Watanabe, K. Hikosaka, T. Matsui, T. Mimura, and S. Hiyamizu, IEEE Electron Device Lett. **25**, 241 (2004).
[2] M. D. Lange, A. Cavus, C. Monier, R. S. Sandhu, T. R. Block, V. F. Gambin, D. J. Sawdai, and A. L. Gutierrez-Aitken, J. Vac. Sci. Technol. B **22**, 1570 (2004).
[3] Y. Zhang, C. S. Whelan, R. Leoni, III, P. F. Marsh, W. E. Hoke, J. B. Hunt, C. M. Laighton, and T. E. Kazior, IEEE Electron Device Lett. **24**, 529 (2003).
[4] R. R. Siergiej, B. Wernsman, S. A. Derry, R. G. Mahorter, R. J. Wehrer, S. D. Link, M. N. Palmisiano, R. L. Messham, S. Murray, C. S. Murray, F. Newman, J. Hills, and D. Taylor, AIP Conf. Proc. **653**, 414 (2003).
[5] M. K. Hudait, Y. Lin, M. N. Palmisiano, and S. A. Ringel, IEEE Electron Device Lett. **24**, 538 (2003).
[6] M. K. Hudait, Y. Lin, D. M. Wilt, F. Wu, J. S. Speck, C. A. Tivarus, E. R. Heller, J. P. Pelz, and S. A. Ringel, Appl. Phys. Lett. **82**, 3212 (2003).
[7] E. A. Fitzgerald, A. Y. Kim, M. T. Currie, T. A. Langdo, G. Taraschi, and M. T. Bulsara, Mater. Sci. Eng., B **67**, 53 (1999).
[8] M. K. Hudait, Y. Lin, M. N. Palmisiano, C. Tivarus, J. P. Pelz, and S. A. Ringel, J. Appl. Phys. **95**, 3952 (2004).
[9] E. A. Fitzgerald, Y.-H. Xie, M. L. Green, D. Brasen, A. R. Kortan, J. Michel, Y.-J. Mii, and B. E. Weir, Appl. Phys. Lett. **59**, 811 (1991).
[10] E. A. Fitzgerald, Y.-H. Xie, D. Monroe, P. J. Silverman, J. M. Kuo, A. R. Kortan, F. A. Thiel, and B. E. Weir, J. Vac. Sci. Technol. B **10**, 1807 (1992).
[11] J. S. Speck, M. A. Brewer, G. Beltz, A. E. Romanov, and W. Pompe, J. Appl. Phys. **80**, 3808 (1996).
[12] R. K. Ahrenkiel and S. W. Johnston, Sol. Energy Mater. Sol. Cells **55**, 59 (1998).
[13] H. Burkhard, H. W. Dinges, and E. Kuphal, J. Appl. Phys. **53**, 655 (1982).
[14] R. K. Ahrenkiel, S. W. Johnston, J. D. Webb, L. M. Gedvilas, J. J. Carapella, and M. W. Wanlass, Appl. Phys. Lett. **78**, 1092 (2001).
[15] J. Crank, *The Mathematics of Diffusion* (Oxford University Press, New York, 1975), Chap. 2.

Downloaded 01 Nov 2005 to 134.134.136.2. Redistribution subject to AIP license or copyright, see http://apl.aip.org/apl/copyright.jsp